JOURNAL OF MATERIALS SCIENCE **37** (2002) 737–744

Sinterability of magnesium silicon nitride powder with yttrium oxide addition coated using the homogeneous precipitation method

K. ITATANI*
Department of Chemistry, Faculty of Science and Engineering, Sophia University, 7-1, Kioi-cho, Chiyoda-ku, Tokyo 102-8554, Japan
E-mail: itatani@sophia.ac.jp

I. J. DAVIES
Advanced Fibro-Science, Kyoto Institute of Technology, Matsugasaki, Sakyo-ku, Kyoto 606-8585, Japan

H. KUWANO, M. AIZAWA
Department of Chemistry, Faculty of Science and Engineering, Sophia University, 7-1, Kioi-cho, Chiyoda-ku, Tokyo 102-8554, Japan

The sinterability of magnesium silicon nitride ($MgSiN_2$) powder with yttrium oxide (Y_2O_3) addition was examined using the hot-pressing technique (31 MPa and N_2 atmosphere) at 1550°C for 90 min; the $MgSiN_2$ powder had been coated with 0–4 mass% of Y_2O_3 addition by a (urea-based) homogeneous precipitation method. Relative densities of the hot-pressed $MgSiN_2$ compacts (ceramics) with and without Y_2O_3 addition were $\geq$99.6% apart for the $MgSiN_2$ceramic with 4 mass% Y_2O_3 addition (98.4%). The thermal conductivities of the $MgSiN_2$ ceramics with 0–1 mass% Y_2O_3 addition were in the range of 20–21 $W \cdot m^{-1} \cdot K^{-1}$ whilst the Vickers hardness was 19.7 GPa for the pure $MgSiN_2$ ceramic and decreased slightly with Y_2O_3 addition. Average fracture toughness values were in the range of 1.2–1.6 $MPa \cdot m^{1/2}$ with significant trend being noted with regards to the ceramic containing 0.5 mass% of Y_2O_3. It was concluded that the use of homogeneous precipitation processing resulted in significant advantages regarding the densification, homogeneous microstructure, and fracture toughness despite the amount of Y_2O_3 addition being as low as 0.5 mass%. *© 2002 Kluwer Academic Publishers*

1. Introduction

The continuing miniaturisation of electronic components has led to calls for a low cost electrical insulation material with high thermal conductivity, κ. The number of potential candidate materials for this role is extremely limited due to the fact that non-metallic crystals with high κ should possess the following characteristics [1]: (i) low atomic mass, (ii) strong inter-atomic bonding, (iii) a simple crystal structure, and (iv) low anharmonicity. One recent candidate material has been that of magnesium silicon nitride ($MgSiN_2$) [1–6], which is predicted to have a theoretical κ value of up to 75 $W \cdot m^{-1} \cdot K^{-1}$ [1] although recent work [6] has indicated an upper limit in the range 27–35 $W \cdot m^{-1} \cdot K^{-1}$. The maximum κ so far achieved has been 25 $W \cdot m^{-1} \cdot K^{-1}$ [2] for the case of hot-pressed material. Further experimental work might provide more insight in the true value of the maximum achievable thermal conductivity for $MgSiN_2$.

The present authors have examined the mechanical and thermal properties of the pressureless-sintered [7] and hot-pressed [8] $MgSiN_2$ compacts (ceramics) containing yttrium oxide (Y_2O_3) as a sintering aid. This sintering aid was selected for promoting the densification of $MgSiN_2$ compact due to the formation of liquid phases at the hot-pressing temperature (1550°C) [7, 8]. The aim of the research was to minimise the amount of Y_2O_3 addition required to fabricate fully dense $MgSiN_2$ ceramics with large average grain sizes and homogeneous microstructure; all of which should maximise κ. The pressureless sintering technique was not able to produce fully dense ceramics [7] and κ was correspondingly low (15–18 $W \cdot m^{-1} \cdot K^{-1}$) as a result of phonon scattering at the numerous voids within the ceramics. However, the hot pressing technique (1550°C/90 min/31 MPa/N_2) [8] achieved almost full density (~99.9%) and a κ value (20–21 $W \cdot m^{-1} \cdot K^{-1}$) only slightly below the maximum so far achieved.

In the present work, the authors have investigated the mechanical and thermal properties of the $MgSiN_2$ ceramics with 0–4 mass% Y_2O_3 addition. The sintering additive (Y_2O_3) was coated onto individual $MgSiN_2$

---

[*] Author to whom all correspondence should be addressed.

particles using a homogeneous precipitation method that has been utilized in the past to coat thin layers (i.e., several nm thick) of sintering aid or, more strictly speaking, sintering aid precursor onto ceramic particles [9, 10]. Use of the homogeneous precipitation method is believed to provide several advantages including the need for reduced amounts of sintering aid, less sever sintering conditions [11], a homogeneous microstructure [11], small grain sizes and improved mechanical properties [12]. Results obtained in this paper were compared with those previously obtained for the $MgSiN_2$ compacts hot-pressed in a N_2 atmosphere under similar conditions [8] except that the Y_2O_3 addition had been mechanically mixed rather than homogeneously precipitated as in the present case.

2. Experimental procedure

The $MgSiN_2$ powder used in this work had been produced by the nitridation of magnesium silicide (Mg_2Si) powder at 1350°C for 10 min. The magnesium silicide was prepared by heating Mg and Si powder compacts (Mg/Si atomic ratios: 2.0 to 3.0, pressure: 50 MPa) at 700°C for 90 min in an Ar atmosphere. Approximately 3.0 g of the $MgSiN_2$ powder was ultrasonically dispersed in 300 cm^3 of deionized water (adjusted to a pH 2–3) together with 0.6 mol of $CO(NH_2)_2$ and an amount of $Y(NO_3)_3 \cdot 6H_2O$ equivalent to 0.5–4 mass% Y_2O_3. The mixed solution was heated to 86°C and held for 60 min, during which time the $CO(NH_2)_2$ was expected to hydrolyze, thus increasing the solution pH and forcing precipitation of Y_2O_3 precursor onto the surfaces of the $MgSiN_2$ particles. Following washing with de-ionized water and drying in air, a dense $MgSiN_2$ ceramic was produced by hot-pressing the coated powder compact with a diameter of 20 mm and thickness of ~2 mm (1.5 g of mass and 30 MPa of pressure) under the optimum conditions for density determined in previous work [8], namely at 1550°C for 90 min in nitrogen (N_2) atmosphere under a uniaxial pressure of 31 MPa. The heating rate was $30°C \cdot min^{-1}$ up to 1100°C and $10°C \cdot min^{-1}$ thereafter to the desired temperature with the ceramic being furnace cooled following the firing process.

Relative density of the ceramic was calculated using the bulk and true densities; the bulk density was determined by measuring the dimensions and mass of each ceramic whereas the true density was determined picnometrically at 25.0°C after pulverizing the ceramic. Crystalline phases within the ceramic were characterised using an X-ray diffractometer (XRD) (Model RAD-IIA, Rigaku, Tokyo) with Ni-filtered CuK_α radiation at 40 kV and 25 mA, and referenced using Joint Committee on Powder Diffraction Standards (JCPDS) cards. The amounts of Mg and Si within the ceramic were determined using an energy dispersive X-ray spectroscope (Link Analytical Pentaflet EDAX system, High Wycombe, UK) with five different readings being averaged for each ceramic. The amounts of oxygen and nitrogen in each ceramic were evaluated using an N/O analyzer (Model TC-136, Leco, St Joseph, MI, USA).

The microstructure of the ceramic was investigated using a field-emission scanning electron microscope (FE-SEM) (Model S-4500, Hitachi, Tokyo; 20 kV accelerating voltage) after coating the surfaces (platinum/palladium) in order to reduce charging effects. The Vickers hardness, H_V, of the ceramic was evaluated using an indentation load, F, and time of 9.8 N and 15 s, respectively (Akashi MVK-E Hardness Tester, Tokyo, Japan), with [13]:

$$H_V = 1.854 \frac{F}{d^2} \tag{1}$$

where d (mm) is the length of the diagonal indent. At least ten different regions were evaluated in order to obtain an average result for each ceramic. An estimate of the fracture toughness, K_{IC}, in the ceramic was carried out by measuring cracks radiating from the indentation tips during hardness testing and utilizing the following equation [14]:

$$K_{IC} = \Psi \left(\frac{E}{H_V} \right)^{\frac{1}{2}} \frac{F}{c^{\frac{3}{2}}} \tag{2}$$

where E is the Youngs modulus (taken to be 279 GPa [15]), c (mm) is the crack length, and $\Psi = 0.016 \pm 0.004$.

The thermal diffusivity of the ceramic was measured using a laser-flash technique on the bulk specimen of size 10 mm × 10 mm × ~1 mm that was cut from the ceramic using a diamond saw. The thermal conductivity was calculated on the basis of the following equation [16]:

$$\kappa = a \rho C_v \tag{3}$$

where a is a thermal diffusivity, ρ is a density, and C_v is a specific heat. A specific heat of $767\ J \cdot kg^{-1} \cdot K^{-1}$ at 300 K was employed in order to calculate the thermal conductivity [17].

3. Results and discussion

3.1. Coating of Y_2O_3 on $MgSiN_2$ particles

When the $MgSiN_2$ particles were coated by sintering aid (Y_2O_3) through a (urea-based) homogeneous precipitation method, $MgSiN_2$ powder had been dispersed in a solution ($CO(NH_2)_2$ and $Y(NO_3)_3$) adjusted to pH 2–3 with the solution pH being easily raised at 86°C by the formation of ammonia due to the hydrolysis of urea. In order to examine the effect of the homogeneous precipitation method on the chemical composition of the $MgSiN_2$ powder, the relationship between Mg/Si atomic ratio for the Mg-Si powder mixture (prior to the preparation of magnesium silicide) and that for the $MgSiN_2$ powder was examined in order to maintain the stoichiometric Mg/Si ratio (=1.0) following homogeneous precipitation processing. The relationship between Mg/Si ratios for the Mg-Si powder mixture and the $MgSiN_2$ powder following homogeneous precipitation has been presented in Fig. 1. Note that, in this case, $Y(NO_3)_3$ was not used during the homogeneous precipitation processing. It can be seen that a Mg/Si ratio of 2.0 for the starting Mg-Si mixture resulted in Mg/Si = 0.96

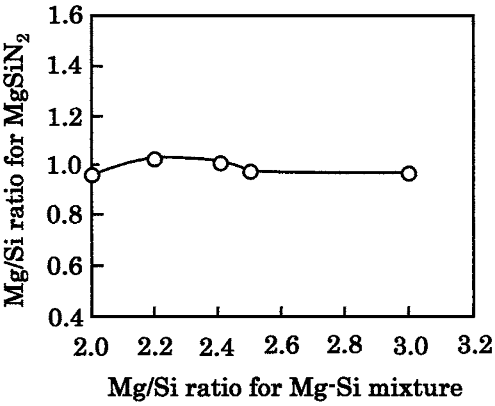

Figure 1 Relationship between Mg/Si ratios for the Mg-Si mixture and $MgSiN_2$ powder (1350°C, 10 min) following homogeneous precipitation processing. Note that homogeneous precipitation processing was conducted without the use of Y_2O_3.

for the $MgSiN_2$ powder. On the other hand, Mg/Si ratios of 2.2 and 2.4 for the Mg-Si powder mixture led to $Mg/Si \simeq 1.02$ for the $MgSiN_2$ powder whilst Mg/Si ratios of 2.5 and 3.0 gave values of $Mg/Si \simeq 0.98$ for the $MgSiN_2$ powder. These data indicated that irrespective of the used Mg/Si ratio the resulting Mg/Si ratio equaled approximately unity.

The present $MgSiN_2$ powder has been prepared by the following two-step routes [18]: (i) preparation of Mg_2Si by the reaction between Mg and Si at 700°C for 90 min (Equation 4) and (ii) the nitridation of Mg_2Si at 1350°C for 10 min (Equation 5).

$$2Mg + Si \rightarrow Mg_2Si \qquad (4)$$

$$Mg_2Si + N_2 \rightarrow MgSiN_2 + Mg\uparrow \qquad (5)$$

When the Mg/Si ratio for the starting Mg-Si powder mixture exceeds stoichiometric value (=1.0) for $MgSiN_2$ (i.e., Mg/Si = 2.0 for Mg_2Si), most of the excess Mg is assumed to have evaporated during the two-step routes, because the Mg/Si ratio for the $MgSiN_2$ powder following homogeneous precipitation was almost stoichiometric. Although there is a possibility that a portion of the residual Mg on the Mg_2Si powder may react with N_2 to form Mg_3N_2 (Equation 6), this Mg_3N_2 also evaporates during heating at 1350°C [18].

$$Mg_3N_2 \rightarrow 3Mg\uparrow + N_2 \qquad (6)$$

Thus no appreciable changes in chemical composition appear to occur for the resulting $MgSiN_2$ powder, regardless of an increase in Mg/Si ratio for the Mg-Si powder mixture. Similar results have also been obtained by Groen *et al.* [5] through the investigation on the chemical compositions and lattice parameters of the $MgSiN_2$ powders, using samples with 5 mol% excess of $MgN_{2/3}$ and 5 mol% excess of $SiN_{4/3}$.

Since the $MgSiN_2$ is known to resist dissolution in mineral acid and alkali solutions [5, 19], no change in chemical composition would be expected to occur during homogeneous precipitation processing. Actually, the average Mg/Si ratio for five kinds of $MgSiN_2$ (see Fig. 1) is 0.99 and the standard deviation of these Mg/Si ratios is 0.022. The Mg/Si ratio for the $MgSiN_2$ at the Mg/Si ratio of 2.0 for the Mg-Si mixture, however, appears to be 0.96 and is slightly lower than other cases. Since there is a possibility that a proportion of "transient" material (e.g., Mg_3N_2) may be dissolved away during homogeneous precipitation processing, it is decided to use a $MgSiN_2$ powder (Mg/Si ratio = 1.02) whose Mg/Si ratio for the Mg-Si powder mixture is 2.2.

3.2. Densification of $MgSiN_2$ with Y_2O_3 addition

The bulk and true (picnometric) densities of the $MgSiN_2$ with no Y_2O_3 addition were 3.098 $g \cdot cm^{-3}$ and 3.120 $g \cdot cm^{-3}$, respectively. The true density increased to 3.171 $g \cdot cm^{-3}$ with increasing amount of Y_2O_3 addition up to 4 mass%. Although the bulk density increased to 3.152 $g \cdot cm^{-3}$ with increasing amount of Y_2O_3 addition up to 3 mass%, it decreased slightly down to 3.120 $g \cdot cm^{-3}$ with a further increase in amount of Y_2O_3 addition up to 4 mass%.

On the basis of the above data, the relative density (i.e., bulk density/true density) of each $MgSiN_2$ ceramic has been presented in Fig. 2 as a function of the amount of Y_2O_3 addition. The starting powder prepared using the homogeneous precipitation method was designated as $MgSiN_2$(HP). It can be seen that, compared to $MgSiN_2$ ceramics whose starting powders had previously been prepared using the mechanical mixing method (designated as $MgSiN_2$(MM)) [8], the present $MgSiN_2$(HP) ceramics possessed relative densities $\geq$99.6% for amounts of Y_2O_3 addition up to 3 mass%. Thus, the coating of Y_2O_3 onto individual $MgSiN_2$ particles contributes to producing dense $MgSiN_2$ ceramics.

A marked difference in relative density was noted for the $MgSiN_2$(HP) and $MgSiN_2$(MM) ceramics with no Y_2O_3 addition. Note that the homogeneous precipitation processing was still conducted (with no Y_2O_3 addition) even for the case of $MgSiN_2$(HP) ceramic. An increased relative density of the $MgSiN_2$(HP) ceramic with no Y_2O_3 addition is, therefore, attributed to the powder adsorbing a larger quantity of OH^- groups during the homogeneous precipitation processing that would be expected to aid densification in the presence

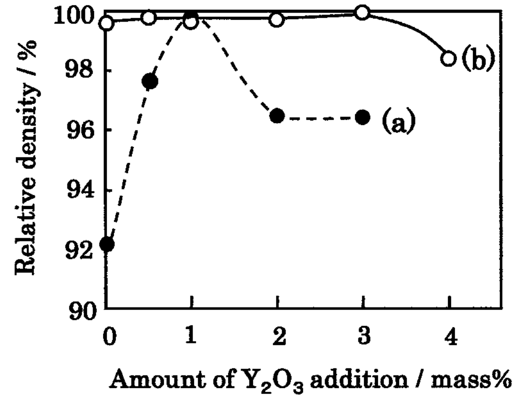

Figure 2 Effect of Y_2O_3 addition on the relative density of (a) $MgSiN_2$(MM) [8] and (b) $MgSiN_2$(HP) compacts hot-pressed at 1550°C for 90 min under a pressure of 31 MPa in a N_2 atmosphere.

of a larger quantity of secondary phases. On the other hand, it is noted that relative densities of the $MgSiN_2$(HP) ceramics with amounts of Y_2O_3 up to 3 mass% were $\geq$99.6%. Since densification of the $MgSiN_2$ ceramic with Y_2O_3 addition is generally promoted by the presence of liquid phases during hot pressing, the present results indicate the contribution of liquid phases to densification to be different between the $MgSiN_2$(HP) and $MgSiN_2$(MM) ceramics. Further details of the liquid phase composition will be described later, together with the FE-SEM and XRD data.

FE-SEM micrographs illustrating the microstructures of the $MgSiN_2$(HP) and $MgSiN_2$(MM) ceramics with 1 mass% Y_2O_3 addition have been shown in Fig. 3. The average grain size of the $MgSiN_2$(MM) ceramic (Fig. 3a) with 1 mass% Y_2O_3 addition was $\sim$0.5 μm whilst that of the $MgSiN_2$(HP) ceramic with 1 mass% Y_2O_3 addition (Fig. 3b) was <0.5 μm. A further difference in microstructure for these two ceramics was that the $MgSiN_2$(MM) ceramic exhibited only equiaxed grains whereas the presence of rod-shaped grains was also noted for the case of the $MgSiN_2$(HP) ceramic (Fig. 3b).

The microstructure of the $MgSiN_2$(HP) ceramic was clearly different compared to that of the $MgSiN_2$(MM) ceramic. In both cases, the liquid phases that are expected to form during hot pressing would assist in the rearrangement of grains, thereby leading to increased densification. In order to discuss the formation temperatures and compositions of the liquid phases, crystalline phases of the $MgSiN_2$(HP) ceramics with Y_2O_3 addition were examined using XRD. Typical XRD results for the $MgSiN_2$(HP) ceramics with and without Y_2O_3 addition have been presented in Fig. 4. The ceramics with no Y_2O_3 addition and with 1 mass% Y_2O_3 addition showed the presence only of $MgSiN_2$ [20] (Fig. 4a and b). The reaction product ($Y_2Si_3O_3N_4$ [21]) could not be detected until the amount of Y_2O_3 addition increased to 4 mass% (Fig. 4c).

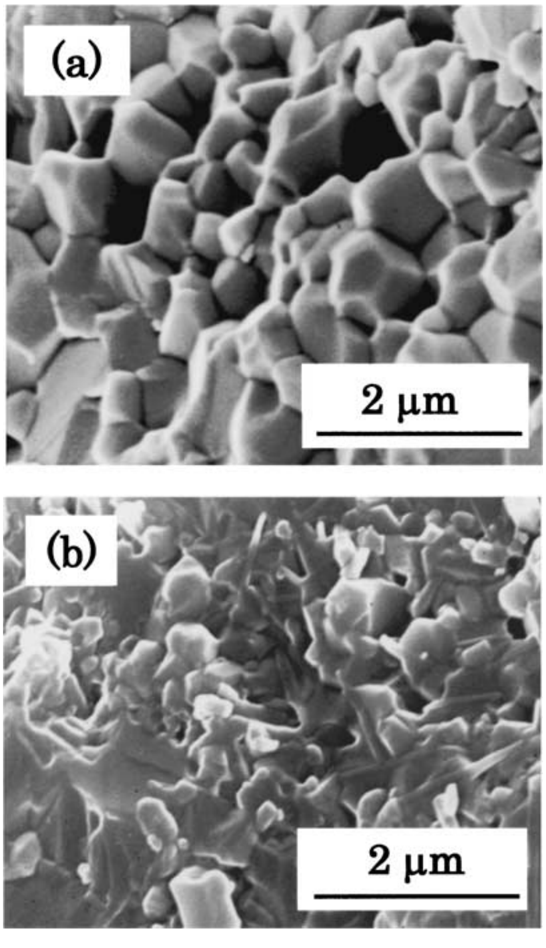

Figure 3 Typical FE-SEM micrographs for the (a) $MgSiN_2$(MM) and (b) $MgSiN_2$(HP) compacts with 1 mass% Y_2O_3 addition hot-pressed at 1550°C for 90 min under a pressure of 31 MPa in a N_2 atmosphere.

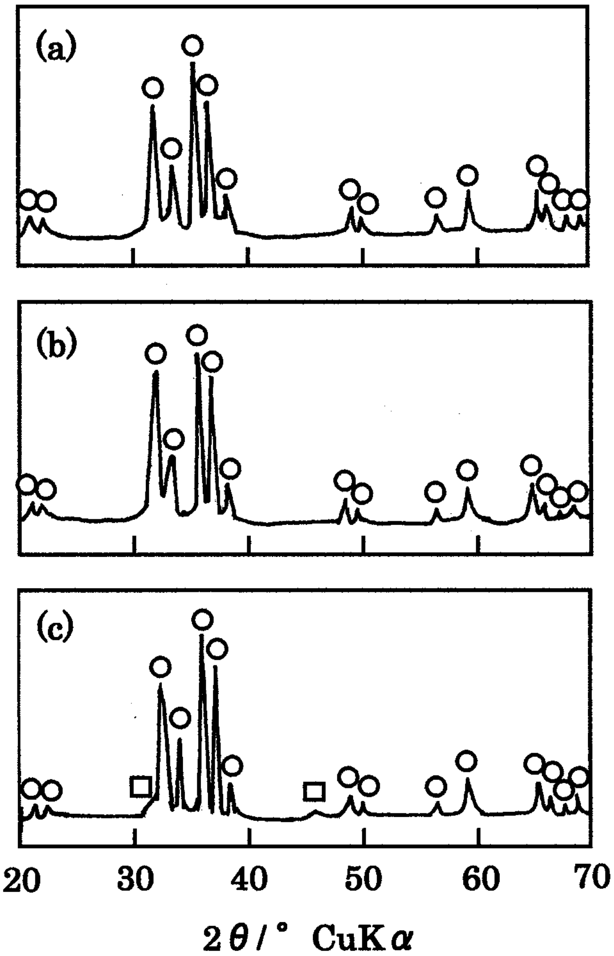

Figure 4 Typical XRD patterns for the $MgSiN_2$(HP) compacts with (a) 0 mass%, (b) 1 mass%, and (c) 4 mass% Y_2O_3 addition hot-pressed at 1550°C for 90 min under a pressure of 31 MPa in a N_2 atmosphere. ○ $MgSiN_2$, □ $Y_2Si_3O_3N_4$.

$Y_2Si_3O_3N_4$ may be formed by the following solid-state reaction:

$$3\mathrm{MgSiN}_2 + \mathrm{Y}_2\mathrm{O}_3 \rightarrow \mathrm{Y}_2\mathrm{Si}_3\mathrm{O}_3\mathrm{N}_4 + \mathrm{Mg}_3\mathrm{N}_2 \qquad (7)$$

Although Mg_3N_2 was not detected by XRD, this is attributed to evaporation during hot pressing as forms of Mg_3N_2 and/or Mg and N_2. Although the relative density of the $MgSiN_2$(HP) ceramic was reduced for the case of 4 mass% Y_2O_3 addition (see Fig. 2), this phenomenon appears to be associated with the formation of a secondary phase ($Y_2Si_3O_3N_4$) which is thermally stable and possesses a high melting point ($\sim$1900°C) [22]. When the Y_2O_3 is partly consumed by the formation of $Y_2Si_3O_3N_4$, as the case of 4 mass% Y_2O_3 addition indicates, the amount of liquid phase appears to be reduced to retard the rearrangement of $MgSiN_2$ grains, thereby retarding densification.

Referring to the liquid compositions, Inomata *et al.* [23] reported a eutectic liquid in the Si_3N_4-$MgSiN_2$ system forms at ~1520°C. Moreover, liquid phases in the Si_3N_4-SiO_2-Y_2O_3-YN system may form at 1550°C [24]. The liquid composition during hot pressing is, therefore, complex and the liquid volume varies according to the amount of Y_2O_3 addition. As for the $MgSiN_2$(MM) ceramic with Y_2O_3 addition, liquid phases in the Si_3N_4-$MgSiN_2$ and Si_3N_4-SiO_2-Y_2O_3-YN systems, which form at the contact points between the $MgSiN_2$ and Y_2O_3 grains, are spread over the grain-boundary region due to capillary forces. The formation routes of liquid phases for the $MgSiN_2$(HP) ceramic with Y_2O_3 addition may be essentially the same as those for the $MgSiN_2$(MM) ceramic. However, since the starting $MgSiN_2$ particles were coated by Y_2O_3 films, the liquid phases formed during hot pressing would appear to spread quickly over the grain-boundary region in order to help rearrangement of the grains towards a more closely packed configuration.

In general, the thermal and mechanical properties of $MgSiN_2$ ceramics may be affected by their chemical composition, in particular the amount of oxygen as an impurity. In order to investigate this, the compositions of $MgSiN_2$(HP) ceramics with and without Y_2O_3 addition were examined quantitatively using EDX. First, the amounts of Mg and Si have been presented in Fig. 5, together with the resulting Mg/Si ratios. Regardless of an increase in Y_2O_3 addition, the amounts of Mg and Si were 29.2–30.6 mass% (theoretical value: 30.23 mass%) and 34.6–36.0 mass% (theoretical value: 34.93 mass%), respectively. Reflecting these results, the Mg/Si ratios for the $MgSiN_2$(HP) ceramics were around unity.

Data illustrating the amounts of nitrogen and oxygen as a function of Y_2O_3 addition have been presented in Fig. 6. The amounts of nitrogen for the $MgSiN_2$(HP) ceramics were in the range of 31.0 to 32.7 mass% (theoretical value: 34.84 mass%), regardless of an increase in the amount of Y_2O_3 addition. The amount of oxygen was maximum (3.03 mass%) for the $MgSiN_2$(HP) ceramic with no Y_2O_3 addition. Although the amount of oxygen decreased to a minimum of 1.19 mass% for the case of 1 mass% Y_2O_3 addition, it increased with a further increase in Y_2O_3 addition and reached 1.84 mass% for the case of 4 mass% Y_2O_3 addition. The maximum amount of oxygen was obtained for the $MgSiN_2$(HP) ceramic with no Y_2O_3 addition.

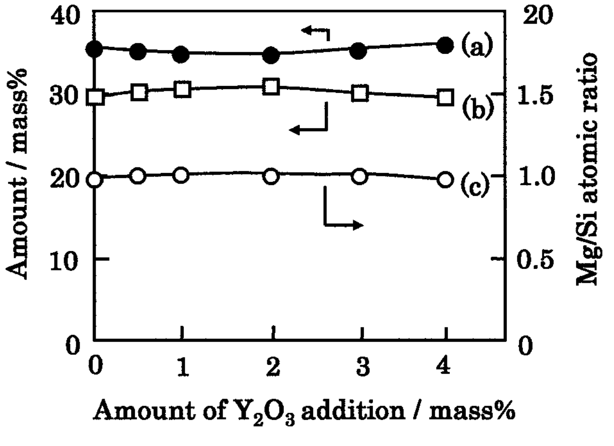

Figure 5 Effect of Y_2O_3 addition on the (a) amount of Si, (b) amount of Mg, and (c) Mg/Si ratio for the $MgSiN_2$(HP) compact hot-pressed at 1550°C for 90 min under a pressure of 31 MPa in a N_2 atmosphere.

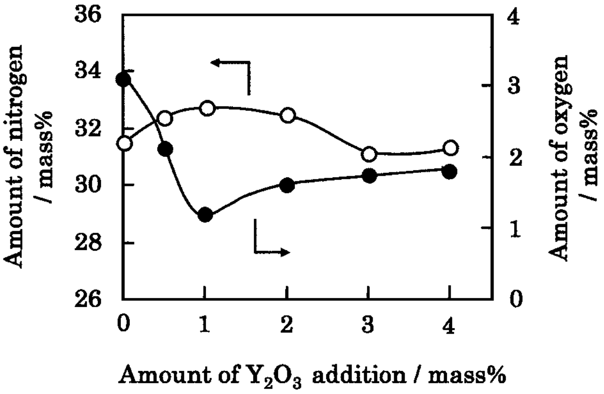

Figure 6 Effect of Y_2O_3 addition on the amounts of nitrogen and oxygen of $MgSiN_2$(HP) compact hot-pressed at 1550°C for 90 min under a pressure of 31 MPa in a N_2 atmosphere.

The presence of oxygen is mainly derived from OH^- groups being adsorbed onto the $MgSiN_2$ particles during the homogeneous precipitation processing. An increase in the amount of oxygen with increasing Y_2O_3 addition is similar to that noted for the $MgSiN_2$(MM) ceramics [8]. Such results are surprising as it might have been reasonable to expect the $MgSiN_2$(HP) ceramics to have possessed a larger amount of oxygen due to the aqueous processing route. The amounts of oxygen determined in the present work are also similar to those encountered by other researchers [25]. Most of the oxygen is not incorporated into the $MgSiN_2$ lattice but instead participates in the formation of secondary phases, because the maximum solubility limit of oxygen into $MgSiN_2$ is on the order of 0.5 mass% [25]. These secondary phases may be present as separate grains in the $MgSiN_2$ matrix [25]. In any case, the presence of oxygen is generally detrimental to the thermal conductivity of $MgSiN_2$ due to the formation of low thermal conductivity phases, e.g., crystalline phase ($Y_2Si_3O_3N_4$) and amorphous phases in the Mg-Si-N-Y-O system [8].

3.3. Thermal properties of $MgSiN_2$ ceramics with Y_2O_3 addition

The relationship between thermal conductivity and amount of Y_2O_3 addition has been shown in Fig. 7. The $MgSiN_2$(HP) ceramic with no Y_2O_3 addition possessed a value of 19.9 $W \cdot m^{-1} \cdot K^{-1}$ whereas the $MgSiN_2$(HP) ceramic with 1 mass% Y_2O_3 addition possessed a maximum value of 20.8 $W \cdot m^{-1} \cdot K^{-1}$. The thermal conductivity of the $MgSiN_2$(HP) ceramic decreased with a further increase in the amount of Y_2O_3 addition and showed a minimum of 18.9 $W \cdot m^{-1} \cdot K^{-1}$ at 4 mass% Y_2O_3 addition.

The thermal conductivity of the $MgSiN_2$(HP) ceramic may also be affected by the location of the

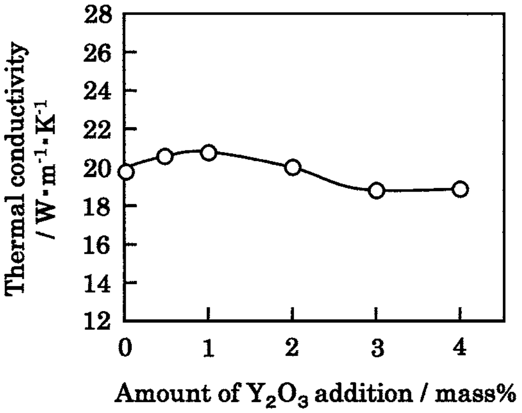

Figure 7 Effect of Y_2O_3 addition on the thermal conductivity of $MgSiN_2$(HP) compact hot-pressed at 1550°C for 90 min under a pressure of 31 MPa in a N_2 atmosphere.

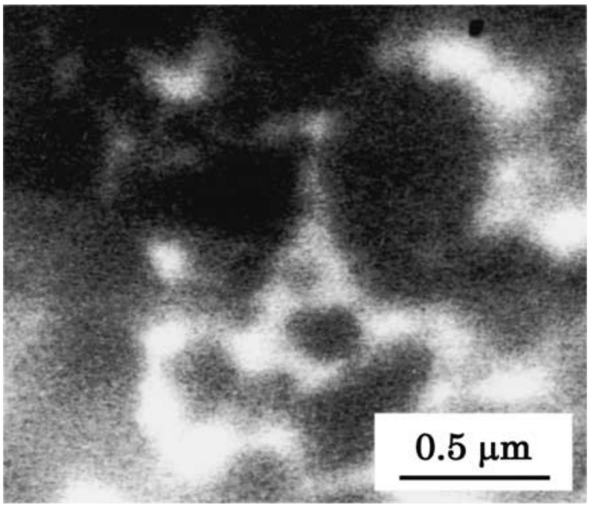

Figure 8 Back-scattering image for the $MgSiN_2$(HP) compact with 4 mass% Y_2O_3 addition hot-pressed at 1550°C for 90 min under a pressure of 31 MPa in a N_2 atmosphere.

crystalline and amorphous phases. In order to check the location of Y-containing reaction products, the backscattered images of $MgSiN_2$(HP) ceramics with Y_2O_3 addition were observed. Typical results of the FE-SEM investigation in backscattered mode for the $MgSiN_2$ ceramic with 4 mass% Y_2O_3 addition have been presented in Fig. 8. This investigation showed evidence of secondary phase grains as indicated by the presence of bright or Y-rich grains and was similar to that noted in previous work [8].

Comparing the thermal conductivity data with the amounts of oxygen, the $MgSiN_2$(HP) ceramic with Y_2O_3 addition possesses higher thermal conductivity as the amount of oxygen is reduced. The maximum thermal conductivity (20.8 $W \cdot m^{-1} \cdot K^{-1}$) of the $MgSiN_2$(HP) ceramic with 1 mass% Y_2O_3 addition is therefore attributed to the smallest amount (1.19 mass%) of oxygen in addition to the high relative density (>99.5%). Nevertheless, the thermal conductivity of $MgSiN_2$ ceramic appears to be less sensitive to the amount of Y_2O_3, compared to the case of AlN ceramics with Y_2O_3 addition [26]. This fact suggests that most of the present reaction products do not hamper the heat transfer between $MgSiN_2$ grains, because they do not coat the $MgSiN_2$ grains but are present as separate grains. Regarding the presence of such separate grains, a recent transmission electron microscopy investigation showed the presence of amorphous phases (as separate grains) at the triple points for sintering aid-free $MgSiN_2$ ceramics with 1.3 mass% oxygen, which is attributed to the poor wetting behaviour of the $MgSiN_2$ grains by the amorphous phases [25].

3.4. Mechanical properties of $MgSiN_2$ ceramics with Y_2O_3 addition

The previous section indicated a clear difference in relative density and grain morphology between the $MgSiN_2$(HP) and $MgSiN_2$(MM) ceramics with Y_2O_3 addition. In this section, the mechanical properties of $MgSiN_2$(HP) ceramics with and without Y_2O_3 addition were compared to those of the $MgSiN_2$(MM) ceramics. The Vickers hardness (H_V) data have been presented in Fig. 9. Values of H_V for the $MgSiN_2$(HP) ceramic were slightly lower, compared to those for the $MgSiN_2$(MM) ceramic [8]. H_V for the pure $MgSiN_2$(HP) ceramic was 19.9 GPa and decreased slightly with Y_2O_3 addition to 17.3 GPa at 4 mass% Y_2O_3 addition.

The trend in H_V is mainly attributed to the increased presence of secondary phases with increasing amount of Y_2O_3 addition. The range of H_V values encountered in the present work (17–21 GPa) is similar to that noted by previous researchers [2].

The effect of Y_2O_3 addition on the fracture toughness (K_{IC}) of $MgSiN_2$(HP) and $MgSiN_2$(MM) [8] ceramics has been presented in Fig. 10. Values of K_{IC} for the $MgSiN_2$(HP) ceramics were similar, or slightly greater, compared to those for the $MgSiN_2$(MM) ceramics [8] and in the range 1.2–1.6 MPa · m$^{1/2}$ with the maximum value being noted for the ceramic with 0.5 mass% Y_2O_3 addition.

It would be reasonable to expect that K_{IC} values may be affected by the microstructure of the $MgSiN_2$ ceramic with Y_2O_3 addition. According to the microstructural observation (see Fig. 3), the $MgSiN_2$(MM) ceramic with Y_2O_3 addition exhibits only equiaxed grains whereas the presence of rod-shaped grains is noted in the $MgSiN_2$(HP) ceramic with Y_2O_3 addition. As the

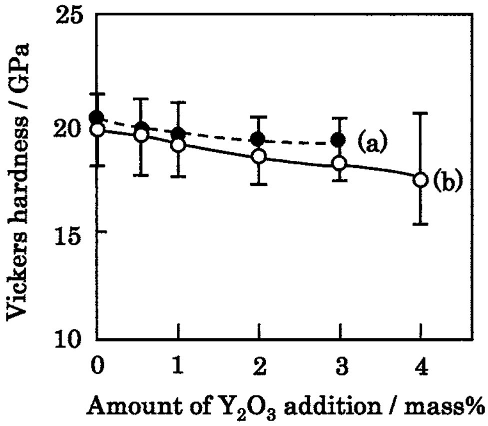

Figure 9 Effect of Y_2O_3 addition on the Vickers hardness of (a) $MgSiN_2$(MM) [8] and (b) $MgSiN_2$(HP) compacts hot-pressed at 1550°C for 90 min under a pressure of 31 MPa in a N_2 atmosphere.

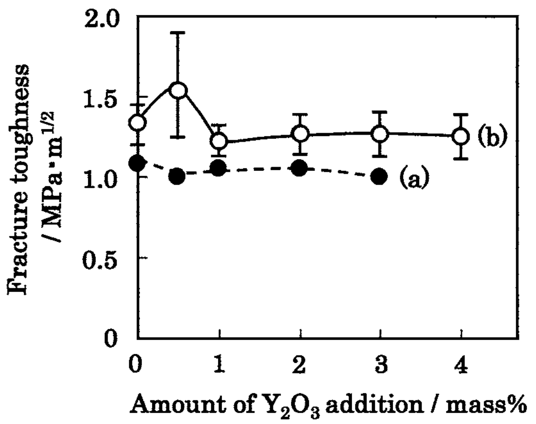

Figure 10 Effect of Y_2O_3 addition on the fracture toughness of (a) $MgSiN_2$(MM) [8] and (b) $MgSiN_2$(HP) compacts hot-pressed at 1550°C for 90 min under a pressure of 31 MPa in a N_2 atmosphere.

FE-SEM observation indicates, the presence of rod-shaped grains in the case of $MgSiN_2$(HP) ceramic with Y_2O_3 addition appears to contribute to the superior fracture toughness in comparison with the case of the $MgSiN_2$(MM) ceramic with Y_2O_3 addition. Data for the present $MgSiN_2$(HP) and $MgSiN_2$(MM) ceramics were, however, both below the previous K_{IC} achieved for $MgSiN_2$ ceramics (3.1–4.4 $MPa \cdot m^{1/2}$ [5]). As the previous $MgSiN_2$ ceramics contained rod-like grains together with a small amount of β-Si_3N_4 [5], the enhancement of fracture toughness appears to be associated with the difference in microstructure.

Overall, it would appear that the significant differences present in relative density and grain morphology of $MgSiN_2$(HP) ceramics had an impact on their fracture toughness characteristics and that the amount of Y_2O_3 addition could be reduced to 0.5 mass%, compared to the case (1 mass%) of $MgSiN_2$(MM) ceramics.

4. Conclusions

The sinterability of magnesium silicon nitride ($MgSiN_2$) powder coated with yttrium oxide (Y_2O_3) addition by a (urea-based) homogeneous precipitation method was examined using a hot-pressing technique (31 MPa and N_2 atmosphere) at 1550°C for 90 min. The results obtained were summarized as follows:

1. The starting $MgSiN_2$ powder was prepared by a two-step routes; (i) the preparation of Mg_2Si by a reaction between Mg and Si, and (ii) nitridation of the Mg_2Si. Although the Mg/Si ratio for the Mg-Si powder mixture varied from 2.0 to 3.0, no appreciable changes in chemical composition occurred for the resulting $MgSiN_2$ powder following the homogeneous precipitation method.

2. Relative densities of the hot-pressed $MgSiN_2$ ceramics with and without Y_2O_3 additions were $\geq$99.6% apart from the $MgSiN_2$ ceramic with 4 mass% Y_2O_3 addition (98.4%). The thermal conductivities of the $MgSiN_2$ ceramics with 0–1 mass% Y_2O_3 addition were in the range of 20–21 $W \cdot m^{-1} \cdot K^{-1}$. A further increase in amount of Y_2O_3 addition slightly reduced the thermal conductivity. The Vickers hardness of the pure $MgSiN_2$ ceramic was 19.7 GPa and it decreased slightly with increasing Y_2O_3 addition. The fracture toughness values were in the range of 1.2–1.6 $MPa \cdot m^{1/2}$ with a maximum value for the 0.5 mass% Y_2O_3 addition.

3. Overall, the use of homogeneous precipitation processing resulted in significant advantages for the densification and homogeneous fine microstructure. The optimum amount of sintering aid was reduced to 0.5 mass% compared to the case (1 mass%) of hot-pressed $MgSiN_2$ ceramics whose starting powders were prepared using the mechanical mixing method.

Acknowledgements

The present authors wish to express their thanks to Mr. S. Tamura (Toshiba Corporation) for measuring thermal diffusivities and to Dr. A. Tsuge (National Industrial Research Institute of Nagoya) for determining the amounts of oxygen and nitrogen of the samples. Furthermore, Dr. H. Uchida (Sophia University) and Dr. R. J. Bruls (Eindhoven University of Technology) are acknowledged for fruitful discussions.

References

1. G. De WITH and W. A. GROEN, in Proceedings of Fourth Euro Ceramics Vol. 3, edited by S. Meriani and V. Sergo (Gruppo Editoriale Faenza Editrice S.p.A., Faenza, Italy, 1995) p. 405.
2. H. T. HINTZEN, R. BRULS, A. KUDYBA, W. A. GROEN and R. METSELAAR, in "Ceramic Transactions Vol. 51: Ceramic Processing Science and Technology," edited by H. Hausner, G. L. Messing and S. Hirano (The American Ceramic Society, Westerville, OH, USA, 1995) p. 585.
3. H. T. HINTZEN, P. SWAANEN, R. METSELAAR, W. A. GROEN and M. J. KRAAN, *J. Mater. Sci. Lett.* **14** (1994) 1314.
4. H. T. HINTZEN, R. BRULS and R. METSELAAR, in Proceedings of Fourth Euro Ceramics Vol. 2, edited by C. Galassi (Gruppo Editoriala Faenza Editrice S.p.A., Faenza, Italy, 1995) p. 289.
5. W. A. GROEN, M. J. KRAAN and G. De WITH, *J. Eur. Ceram. Soc.* **12** (1993) 413.
6. R. J. BRULS, Ph.D. Thesis (CIP-DATA Library Technische Universiteit Eindhoven (Eindhoven University of Technology, Eindhoven, The Netherlands, 2000) p. 177.
7. I. J. DAVIES, H. UCHIDA, M. AIZAWA and K. ITATANI, *J. Soc. Inorg. Mater., Japan* **6** (1999) 40.
8. I. J. DAVIES, T. SHIMAZAKI, M. AIZAWA, H. SUEMASU, A. NOZUE and K. ITATANI, *ibid.* **6** (1999) 276.
9. A. K. GARG and L. C. De JONGHE, *J. Mater. Res.* **5** (1990) 136.
10. I. J. DAVIES, B. DJURICIC, S. PICKERING and J. TH. M. De HOSSON, *J. Surf. Anal.* **3** (1997) 394.
11. A. BELLOSI and G. N. BABINI, *Key Eng. Maters.* **161–163** (1999) 203.
12. C. M. WANG, *J. Maters. Sci.* **31** (1996) 4709.
13. B. R. LAWN and D. B. MARSHALL, *J. Amer. Ceram. Soc.* **62** (1979) 347.
14. G. R. ANSTIS, P. CHANTIKUL, B. R. LAWN and D. B. MARSHALL, *ibid.* **64** (1981) 533.
15. R. J. BRULS, Ph.D. Thesis (CIP-DATA Library Technische Universiteit Eindhoven (Eindhoven University of Technology, Eindhoven, The Netherlands, 2000) p. 137.
16. D.-M. LIU, C.-J. CHEN and R. R. R. LEE, *J. Appl. Phys.* **77** (1995) 494.
17. R. J. BRULS, H. T. HINTZEN, R. METSELAAR and J. C. VAN MILTENBURG, *J. Phys. Chem.* B **102** (1998) 7871.
18. H. UCHIDA, K. ITATANI, M. AIZAWA, F. S. HOWELL and A. KISHIOKA, *J. Ceram. Soc. Japan* **105** (1997) 934.
19. J. DAVID and J. LANG, *C. R. Acad. Sci. Paris* **261** (1965) 1005.

20. Powder Diffraction File Card No. 25-530, JCPDS International Center for Diffraction Data, Newton Square, PA (1975).
21. Powder Diffraction File Card No. 45-249, JCPDS International Center for Diffraction Data, Newton Square, PA (1995).
22. K. H. JACK, *J. Mater. Sci.* **11** (1976) 21.
23. Y. INOMATA, K. YUKINO, T. MATSUNAGA and T. WADA, *Yogyo-Kyokai-Shi* **84** (1976) 534.
24. L. J. GAUKLER, H. HOHNKE and T. Y. TIEN, *J. Amer. Ceram. Soc.* **63** (1980) 35.
25. R. J. BRULS, Ph.D. Thesis (CIP-DATA Library Technische Universiteit Eindhoven (Eindhoven University of Technology, Eindhoven, The Netherlands, 2000) p. 59.
26. P. S. BARANDA, A. W. KNUDSEN and E. RUH, *J. Amer. Ceram. Soc.* **77** (1994) 1846.

Received 28 February
and accepted 2 October 2001